Biogeochemistry
https://doi.org/10.1007/s10533-022-00906-y

From canopy to consumer: what makes and modifies terrestrial DOM in a temperate forest

M. I. Behnke · J. B. Fellman · D. V. D'Amore · S. M. Gomez · R. G. M. Spencer

Received: 27 July 2021 / Accepted: 9 February 2022
© The Author(s), under exclusive licence to Springer Nature Switzerland AG 2022

Abstract To investigate how source and processing control the composition of "terrestrial" dissolved organic matter (DOM), we combine soil and tree leachates, tree DOM, laboratory bioincubations, and ultrahigh resolution Fourier-transform ion cyclotron resonance mass spectrometry in three common landscape types (upland forest, forested wetland, and poor fen) of Southeast Alaska's temperate rainforest. Tree (*Tsuga heterophylla* and *Picea sitchensis*) needles and bark and soil layers from each site were leached, and tree stemflow and throughfall collected to examine DOM sources. Dissolved organic carbon concentrations were as high as 167 mg CL^{-1} for tree DOM, suggesting tree DOM fluxes may be substantial given the hypermaritime climate of the region. Condensed aromatics contributed as much as 38% relative abundance of spruce and hemlock bark leachates suggesting coniferous trees are potential sources of condensed aromatics to surface waters. Soil leachates showed soil wetness dictates DOM composition and processing, with wetland soils producing more aromatic formulae and allowing the preservation of traditionally biolabile, aliphatic formulae. Biodegradation impacted soil and tree DOM differently, and though the majority of source-specific marker formulae were consumed for all sources, some marker formulae persisted. Tree DOM was highly biolabile (> 50%) and showed compositional convergence where processing homogenized DOM from different tree sources. In contrast, wetland and upland soil leachate DOM composition diverged and processing diversified DOM from different soil sources during bioincubations. Increasing precipitation intensity predicted

Responsible Editor: Penny Johnes.

Supplementary Information The online version contains supplementary material available at https://doi.org/10.1007/s10533-022-00906-y.

M. I. Behnke (✉) · R. G. M. Spencer
National High Magnetic Field Laboratory Geochemistry Group and Department of Earth, Ocean, and Atmospheric Science, Florida State University, Tallahassee, FL, USA
e-mail: mibehnke@fsu.edu

R. G. M. Spencer
e-mail: rgspencer@magnet.fsu.edu

J. B. Fellman
Department of Natural Sciences and Alaska Coastal Rainforest Center, University of Alaska Southeast, Juneau, AK, USA
e-mail: jbfellman@alaska.edu

D. V. D'Amore
USDA Forest Service, Pacific Northwest Research Station, Juneau, AK, USA
e-mail: david.v.damore@usda.gov

S. M. Gomez
Department of Biological Sciences, Florida State University, Tallahassee, FL, USA
e-mail: smg19a@my.fsu.edu

Published online: 02 March 2022

with climate change in Southeast Alaska will increase tree leaching and soil DOM flushing, tightening linkages between terrestrial sources and DOM export to the coastal ocean.

Keywords Dissolved organic matter · FT-ICR MS · Tree DOM · Soil DOM · Microbial processing · Condensed aromatics

Introduction

The composition and thus ecological role of dissolved organic matter (DOM) is controlled by its source and processing history along the terrestrial-aquatic continuum (Antony et al. 2017; Hansen et al. 2016; Shirokova et al. 2019; Wagner et al. 2019b). Precipitation interacts with forest vegetation and soil, leaching DOM from multiple sources along its flowpath to form terrestrially-sourced allochthonous DOM. Precipitation first encounters tree canopies, where it can flow down tree trunks as stemflow or pass through branches as throughfall, accruing "tree DOM" sourced from a combination of deposition, microbial metabolites, and plant-derived molecules (Guggenberger et al. 1994; Van Stan and Stubbins 2018). Precipitation that is not intercepted by tree canopies either runs off the landscape as surface flow without interaction with soil organic matter, or infiltrates into soils and leaches DOM along soil flowpaths (D'Amore et al. 2012; Inamdar et al. 2012). Riverine DOM composition can shift with changing source contributions, demonstrating the importance of source to DOM character (Behnke et al. 2020; Kurek et al. 2021; Wagner et al. 2019b). However, microbial processing in headwater streams can also homogenize DOM before it reaches watershed outlets, minimizing the relevance of specific DOM sources to overall DOM composition (Harfmann et al. 2019; Rossel et al. 2013). Elucidating the balance between microbial homogenization and source specificity in dictating DOM composition will allow us to better assess the importance of terrestrial DOM source in dictating DOM chemistry.

The Northeast Pacific Coastal Temperate Rainforest (NPCTR) of Southeast Alaska provides an ideal location in which to assess the impacts of source versus processing on terrestrial DOM composition. The annual land-to-ocean flux of dissolved organic carbon (DOC) from Southeast Alaskan watersheds is massive, and currently equates to ~ 20% the flux from the entire contiguous United States due to the high DOC yield (Edwards et al. 2021). Further, soil and tree biomass in the NPCTR contain substantial carbon stocks (Buma et al. 2016; Heath et al. 2011; McNicol et al. 2019) and temperate rainforests such as the NPCTR have the highest carbon density of any forest ecosystem (Keith et al. 2009), providing sizable and varied carbon sources for DOM leaching. Southeast Alaskan landscapes experience substantial precipitation, with precipitation intensity projected to increase with climate change, potentially influencing the magnitude of DOM fluxes to the productive coastal ocean (Bidlack et al. 2021; Lader et al. 2020; Nash et al. 2018). Rain and subsequent runoff allow leaching and transportation of carbon from sources to streams as DOM. The balance of source identity versus microbial processing in dictating DOM composition remains unclear but is a critically important component of regional carbon biogeochemistry.

Here we use ultrahigh resolution Fourier-transform ion cyclotron resonance mass spectrometry (FT-ICR MS) to examine DOM composition from common terrestrial carbon sources to NPCTR watersheds. We further pair FT-ICR MS with laboratory bioincubations to determine how microbial processing impacted the chemical composition of the following tree and soil endmember sources: (1) soil leachates in the three most prevalent landscape units (poor fen, forested wetland and upland forest) in the NPCTR (D'Amore et al. 2015a; McNicol et al. 2019); (2) leachates from western hemlock (*Tsuga heterophylla*) and Sitka spruce (*Picea sitchensis*), which are the two dominant tree species in the NPCTR; and 3) stemflow and throughfall (hereafter, "tree DOM") of spruce and hemlock. We assess whether specific DOM sources contain unique chemical signatures and whether sources retained compositionally distinct DOM signatures after microbial modification.

Methods

Site description

Sampling took place in Aangoo̲a Yé (referred to in past studies as Fish Creek) watershed near Juneau, Alaska (Fig. 1; D'Amore et al. 2015a). Sampling

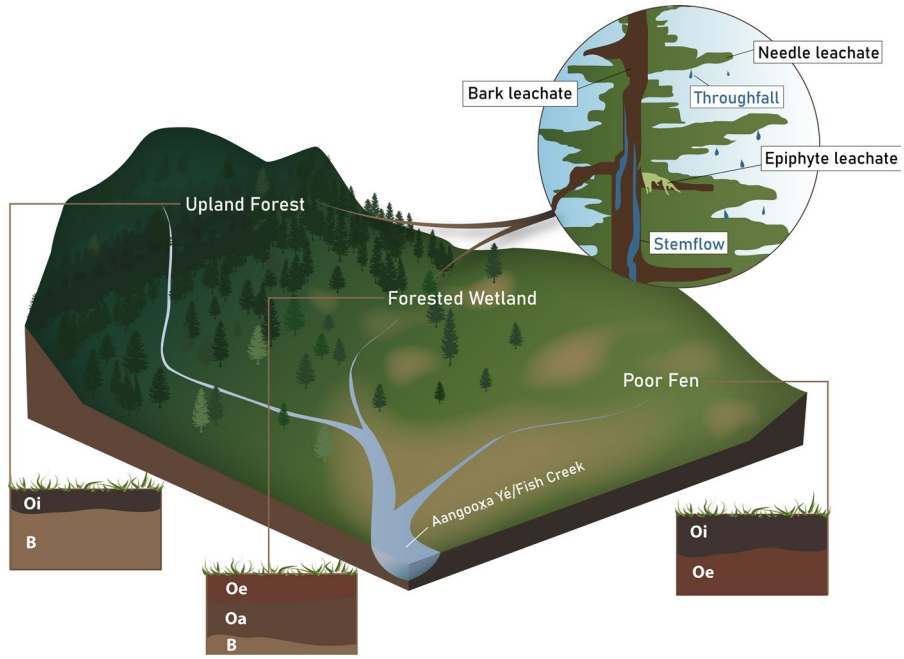

Fig. 1 Sampling design for the three landscape types in Aangooxa Yé/Fish Creek watershed near Juneau, Alaska. Soil layers for upland forest, forested wetland, and poor fen are shown. Both spruce and hemlock were sampled for bark and needle leachates (along with a combined epiphyte leachate), stemflow, and throughfall

occurred during the snow-free period in order to capture terrestrial DOM sources during the main runoff period including spring snowmelt (May) and summer water table draw-down (June to early August) (Fellman et al. 2009a). Aangooxa Yé and its sub-catchments have previously been established as a hydropedologic observatory (D'Amore et al. 2012), and the hydrology, biogeochemistry, and soil carbon dynamics of these catchments have been extensively studied for the past decade (e.g. D'Amore et al. 2015a; Fellman et al. 2008, 2020). The area has a moderate maritime climate with cool summers, mild winters, and substantial precipitation (~2,000 mm at sea level). Aangooxa Yé watershed (36 km^2; 487 m mean elevation) contains coniferous forest, forested wetlands, emergent wetlands, and alpine areas that seasonally accumulate snow that persists throughout much of the summer.

The three study landscape types have specific hydrodynamics that impact carbon accumulation and flux in the NPCTR. Poor fens (fen) cover ~ 9% of the NPCTR and are a largely unforested and poorly-drained wetland type (D'Amore et al. 2015a; National Wetlands Working Group 1988). The poor fen sub-catchment has organic soils classified as Typic Cryohemists that are acidic (pH < 4.0) with peat accumulation of > 2 m, and a vegetation community that contains Sphagnum mosses (*Sphagnum* spp.), shore pine, ericaceous shrubs, and sedges (Fellman et al. 2008). It has a mean elevation of 253 m, a mean slope of 6.6%, and an estimated soil C stock of 556 Mg C ha^{-1} to 2 m deep (D'Amore et al. 2015a).

Forested wetlands cover ~ 12% of the NPCTR (D'Amore et al. 2015a). The forested wetland sub-catchment contains organic soils classified as Terric Cryohemists with acidic (pH < 4.0) peat 0.50–0.75 m deep overlying glacial till (Fellman et al. 2008), and is characterized as a raised peatland swamp (National Wetlands Working Group 1988). The forested wetland contains vegetation communities with Sphagnum mosses, blueberry (*Vaccinium* spp.), and skunk cabbage (*Lysichiton americanum*) beneath an overstory of western hemlock and Sitka spruce. The hydrodynamics of the forested wetland and poor fen differ in both the seasonality and conductivity of the surface organic layers, but soils in both show oscillating aerobic and anaerobic conditions (D'Amore et al. 2010, 2015a). The sub-catchment has a mean elevation of 240 m, a mean slope of 15.5%, and an estimated soil carbon content of 376 Mg C ha^{-1} in the organic layers (D'Amore et al. 2015a).

Upland forests cover ~ 78% of the NPCTR. The upland forest sub-catchment has soils classified as Typic Haplocryods with acidic organic matter

over colluvial material on steep slopes with a mean elevation of 392 m, a mean slope of 19.4%, and an estimated soil carbon content of 245 Mg C ha^{-1} to 0.80 m deep (D'Amore et al. 2015a; Fellman et al. 2008). Upland forest vegetation is also primarily blueberry, western hemlock, and Sitka spruce.

Tree DOM collection

Tree DOM samples were collected for analyses from a storm in both June (the first large rain event after the watershed was not subject to snow and ice on branches) and August to capture event variability from the upland and forested wetland following an adaptation of previously published methods (Stubbins et al. 2017). All glassware for tree DOM collection was pre-cleaned (pH 2 ultrapure water bath; ultrapure water rinsing; combusted for > 4 h at 450 °C) prior to deployment. Twenty-four glass throughfall collectors were placed under 12 trees (three spruce and three hemlock at each of the forested wetland and upland sites). An additional two glass collectors were placed in a nearby unforested site to collect rainfall. Stemflow samplers consisted of precleaned collars cut from (acid leached and ultrapure water rinsed) polyethylene tubing installed on each tree circling the trunk ~ 1.5 m from the ground. Precleaned glass sampling containers were attached to each tubing collar outflow at the time of deployment before the storms. After each rain event, sample volumes were measured. Concentrations of DOC were measured (see below for method) for each tree DOM sample separately when sample volumes allowed and composited by sample type when volumes were too small. Tree DOM samples from the first storm sampling were composited by tree species, catchment, and sample type for FT-ICR MS and stored frozen in precleaned (acid-rinsed) polycarbonate bottles until extraction. Sample volumes from the only sampled August storm large enough to sample for DOC concentration during the field season were too small to allow FT-ICR MS analysis or bioincubations.

Tree leachates

Tree leachate samples were collected twice to match tree DOM collection, in June and August, and leached using an adaptation of previously detailed methods (Johnston et al. 2019; Textor et al. 2019). Needles and bark from three hemlock and three spruce trees in both the forested wetland and upland sub-catchments were collected by clipping branches, bark, and foliage. Samples were composited by tree species, sample type, and catchment. Epiphytes (lichens and moss) from both tree species and catchments were collected and composited as an epiphyte sample type. All tree leachate samples were oven-dried at 50 °C for 24 h. Dried samples were placed in 500 g of Milli-Q water in acid-cleaned polycarbonate bottles and left to leach in the dark for 3 h (Table S1).

Soil layer characterization, collection, and leachates

Soil sampling occurred twice, in spring (May) and late summer (August). A soil pit was excavated at each site and soil genetic horizons were delineated that corresponded to previously characterized pedons in close proximity at the site (see D'Amore et al. 2015a). In the poor fen, soil samples were collected from the O_i (~ 0–10 cm deep) and O_e horizon (~ 10–50 cm deep). In the forested wetland, the O_e (~ 5–25 cm deep), O_a (~ 25–45 cm deep), and a B horizon (~ 45–70 cm deep; B_w) were sampled. In the upland forest, the O_i (~ 0–10 cm deep), and a B horizon (~ 20–45 cm deep; B_s) were sampled. Samples were returned to the laboratory where 40 g dry weight of each soil horizon as leached in a 0.001 M $NaHCO_3$ solution (prepared with ultrapure water) for 24 h on a shaker table in the dark (Textor et al. 2019).

DOC measurements and biodegradable DOC

Samples for DOC from all water sources were filtered through pre-combusted (> 4 h at 450 °C) Whatman GF/F filters (0.7 µm pore size) and stored refrigerated in sample rinsed and pre-combusted (> 4 h at 550 °C) amber glass vials or acid-cleaned polycarbonate bottles until analysis within 48 h of collection (Stubbins and Dittmar 2012). For soil leachates, water was initially prefiltered through a Whatman GF/D filter (pre-combusted > 4 h at 450 °C; 2.7 µm pore size). Concentrations of DOC were determined via non-purgeable organic C analysis on a Shimadzu TOC-LC/TN analyzer. Samples were acidified and sparged to remove inorganic C followed by high-temperature combustion and analysis on the TOC analyzer (Stubbins and Dittmar 2012). Biodegradable DOC (BDOC) of leachates and tree DOM were calculated

as the difference in DOC concentration before and after a 14-day incubation expressed as a percent loss of DOC (Textor et al. 2019). Triplicate filtered (> 4 h at 450 °C 0.7 µm Whatman GF/F) leachates and samples were amended with a 1% microbial inoculum (made by filtering leachate water through 2.7 µm GF/D filters) and were nutrient amended based on doubled Redfield ratios of inorganic nitrate and phosphate (KNO_3 and Na_2HPO_4; 106C:32 N:2P). Thus, nutrients were added to each sample in equal proportions based on the initial DOC concentration of each sample to prevent nutrient limitation during the incubations (Howard et al. 2018; Vonk et al. 2015). Incubations were kept in the dark on a shaker table at 20 °C with lids cracked to allow oxygen exchange. After 14 days, aliquots were re-filtered and DOC measured for the end time point.

Fourier-transform ion cyclotron resonance mass spectrometry

Aliquots for FT-ICR MS analysis were frozen in pre-cleaned polycarbonate bottles until extraction. Solid-phase extraction of samples was conducted using reverse phase Bond Elut Priority PolLutant (PPL) columns (100 mg; Agilent) (Dittmar et al. 2008). Carbon normalized volumes of acidified (pH 2) samples (40 µg C mL^{-1} target concentrations for JT Baker HPLC grade methanol elutes) were passed through pre-cleaned PPL columns. Elutes were stored at -20° C until analysis on a custom-built FT-ICR MS equipped with a passively shielded 9.4 T magnet (Oxford Instruments, Abington, Oxfordshire, U.K.) at the National High Magnetic Field Laboratory (Tallahassee, Florida, U.S.A.; Kaiser et al. 2011; Stenson et al. 2003) with direct infusion negative electrospray ionization. Each mass spectrum collected consisted of 100 coadded time domain acquisitions. Since extraction and ionization are not 100% efficient, FT-ICR MS spectra provide data on the extracted and ionized fraction of the DOM pool and cannot be assumed to capture all formulae present in DOM samples.

Molecular formulae were assigned to peaks with > 6σ root-mean-square baseline noise with previously described guidelines (Koch et al. 2007) with PetroOrg ©™ software (Corilo 2015). Formulae assignment boundaries were $C_{1\text{-}45}H_{1\text{-}92}N_{0\text{-}4}O_{1\text{-}25}S_{0\text{-}2}$ and a mass accuracy ≤ 300 ppb (Kellerman et al. 2018). The modified aromaticity index (AI_{mod}; used to assess the degree of unsaturation based on molecular formula) was calculated (Koch and Dittmar 2006, 2016). Compound classes were defined using AI_{mod} and elemental ratios as follows: polyphenolics ($0.5 < AI_{mod} \leq 0.66$); condensed aromatics ($AI_{mod} > 0.66$); highly unsaturated and phenolic ($AI_{mod} \leq 0.5$, $H/C < 1.5$, $O/C \leq 0.9$; HUPs); aliphatics ($1.5 \leq H/C \leq 2.0$, $O/C \leq 0.9$ and $N = 0$); N-containing aliphatic compounds (also known as peptide-like formulae; $1.5 \leq H/C \leq 2.0$, $O/C \leq 0.9$ and $N > 0$); and sugar-like ($O/C > 0.9$). Though unique molecular formulae can be assigned to FT-ICR MS peaks, each formula can represent numerous structural isomers (Hertkorn et al. 2007). Therefore, the term "compound" refers to the different compounds the formulae represent rather than a specific isomer and is used in reference to compound classes only. Relative abundances of each formula were determined by normalizing each peak magnitude to the sum of all assigned peaks in each sample. The contributions of the compound classes were then calculated as the sum of all the relative abundances of each peak in each compound class divided by the summed abundances of all assigned formulae in each sample expressed as percentages. Similar calculations were used to determine the relative abundances of compounds containing different elemental compositions (e.g. CHO, CHON, CHOS, CHONS).

Bioconsumed/bioproduced molecular formulae were identified as formulae that were present or absent in the analytical window above > 6σ root-mean-square baseline noise in all initial bioincubation spectra for a DOM source (e.g. hemlock throughfall) and similarly absent or present in all final bioincubation spectra for that DOM source, due to a combination of biological processes and any potential changes in ionization. Unique marker formulae were identified as formulae that appeared in all initial spectra for a given DOM source and in none of the samples for the comparable DOM sources. For example, formulae unique to spruce stemflow DOM appeared in all initial spruce stemflow spectra and none of the initial samples for other DOM sources, be they soil leachates or other tree samples.

Statistical analyses

In our study, we performed three statistical comparisons: (1) between soil leachate DOM from the

three landscape types; (2) between spruce and hemlock sourced DOM; and (3) between needle and bark DOM. Our goal for sampling in both May/June and August was to increase our sample size for the DOM composition analyses rather than evaluate seasonal patterns in DOM composition. Bioincubations allowed us to examine the changes occurring to DOM during microbial processing, which causes the majority of annual carbon dioxide emissions from DOM at these latitudes and contributes more to DOM degradation than does photochemistry in short, shaded streams (Groeneveld et al. 2016; Koehler et al. 2014). Differences in tree DOM between needle and bark leachates, tree species, and tree DOM type were tested with Welch two-samples *t*-tests in R (R Core Team 2019) using *rstatix* (Kassambara 2020). Kruskal–Wallis tests and Wilcoxon's tests to assess differences between soil leachates in the three sub-catchments were performed in R. Principal component analysis (PCA) was used to examine relationships between FT-ICR MS compound and heteroatomic classes in R (R Core Team 2019) using the *ggfortify* package (Horikoshi and Tang 2016; Tang et al. 2016) with variables scaled to unit variance to make them comparable. This technique reduces continuous multivariate data dimensionality while retaining information on dataset variability.

Results

DOC concentration and DOM composition

Canopy, trunk, and soil DOM sources varied in concentration and biolability of DOC and in FT-ICS MS data bulk metrics (Fig. 2; Table 1), and compound class and heteroatom class relative abundances (Fig. 3; Table 2). Concentrations of DOC in the full suite of tree DOM samples ranged from 22.9 ± 3.3 mg CL^{-1} in hemlock throughfall to 88.7 ± 19.5 mg CL^{-1} in spruce stemflow (Table 1) with maximum values of 66 and 167 mg CL^{-1} for spruce throughfall and stemflow samples. Concentrations of DOC were on average greater in stemflow than throughfall samples ($t_{4.39} = 4.56$, $p < 0.01$; Fig. 2; Table S2 for statistics). Rainfall DOC concentrations were minimal (0.5 ± 0.0 mg CL^{-1}) indicating precipitation did not noticeably contribute to tree DOM

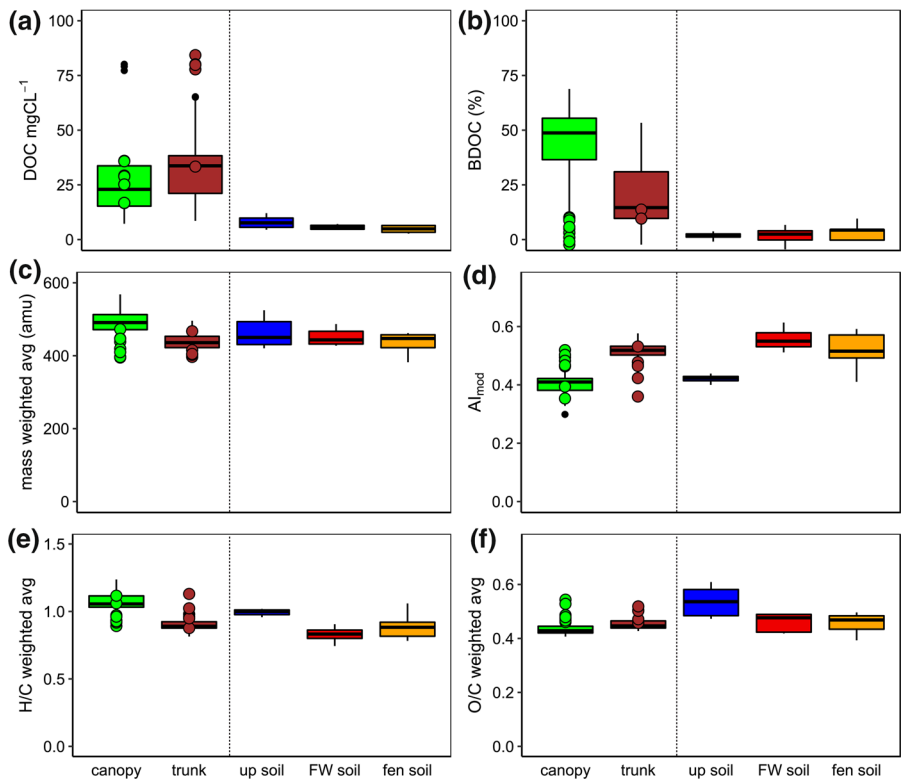

Fig. 2 Canopy (throughfall and needle leachates), trunk (stemflow and bark leachates), forested wetland (FW), fen, and upland DOC concentrations and FT-ICR MS bulk metrics. Throughfall and stemflow values are indicated by the colored points in the canopy and trunk categories; those boxes represent needle and bark leachate data. The median is represented by a horizontal line, boxes extend to the 25th and 75th percentiles, and whiskers extend to the minimum or maximum value or 1.5 times the interquartile range past the box (whichever is nearer the median). The black dots are outlying points past the whiskers' range

Table 1 DOC concentrations, %BDOC, number of samples per grouping, and bulk FT-ICR MS metrics for soil leachates, tree leachates, and tree DOM (stemflow and throughfall) initial (main sample) and final timepoints

Catchment/position		i/f[a]	n for bulk	DOC (mg CL^{-1})	%BDOC	n for FT-ICR MS	Mass weighted average (Da)	O/C	H/C	AI_{mod}
Tree DOM sample (stemflow and throughfall)										
Rain		i	3	0.5 ± 0.0	21.3 ± 1.5	1	371.6	0.40	1.38	0.25
		f	3	0.4 ± 0.0						
Spruce throughfall		*	12	31.1 ± 4.3						
		i	6	30.6 ± 2.4	0.8 ± 0.9	2	447.0 ± 0.4	0.47 ± 0.01	0.97 ± 0.01	0.47 ± 0.00
		f		30.2 ± 2.2		2	428.8 ± 9.4	0.49 ± 0.03	1.03 ± 0.09	0.42 ± 0.07
Spruce stemflow		*	7[b]	88.7 ± 19.5						
		i	3	79.2 ± 0.7	11.0 ± 1.0	2	403.7 ± 1.3	0.51 ± 0.01	1.08 ± 0.05	0.39 ± 0.03
		f		70.6 ± 0.6		2	409.0 ± 6.3	0.46 ± 0.00	0.93 ± 0.05	0.50 ± 0.03
Hemlock throughfall		*	12	22.9 ± 3.3						
		i	6	22.9 ± 2.8	8.2 ± 0.9	2	441.1 ± 31.4	0.48 ± 0.01	0.92 ± 0.00	0.49 ± 0.01
		f		20.9 ± 2.4		2	395.8 ± 0.8	0.52 ± 0.03	0.98 ±	0.46 ± 0.06
Hemlock stemflow		*	3[c]	39.4 ± 24.3						
		i	2	58.8 ± 14.7	n/a	2	431.9 ± 35.2	0.49 ± 0.02	1.00 ± 0.01	0.47 ± 0.01
Tree leachates										
Epiphyte		i	6	33.6 ± 0.6	40.9 ± 4.4	2	485.5 ± 12.9	0.49 ± 0.01	1.02 ± 0.00	0.42 ± 0.00
		f	6	20.0 ± 1.9		1	463.1	0.47	1.01	0.44
Spruce needles		i	12	26.5 ± 2.4	56.0 ± 3.2	4	487.3 ± 25.1	0.44 ± 0.01	1.13 ± 0.05	0.36 ± 0.03
		f	12	11.8 ± 1.6		2	490.0 ± 6.4	0.41 ± 0.00	1.07 ± 0.01	0.41 ± 0.00
Spruce bark		i	12	24.3 ± 4.2	12.2 ± 0.8	4	442.3 ± 10.0	0.45 ± 0.01	0.91 ± 0.02	0.51 ± 0.01
		f	12	21.6 ± 3.8		2	410.1 ± 15.8	0.43 ± 0.01	0.93 ± 0.00	0.51 ± 0.01
Hemlock needles		i	12	30.6 ± 8.7	36.7 ± 3.7	4	520.0 ± 17.3	0.44 ± 0.01	1.02 ± 0.0	0.43 ± 0.02
		f	12	21.6 ± 6.6		2	422.7 ± 27.4	0.43 ± 0.01	1.09 ± 0.04	0.40 ± 0.02
Hemlock bark		i	12	37.2 ± 5.5	10.4 ± 1.6	4	443.2 ± 18.9	0.46 ± 0.01	0.85 ± 0.02	0.54 ± 0.02
		f	12	32.8 ± 4.6		2	451.2 ± 7.8	0.47 ± 0.00	0.88 ± 0.01	0.52 ± 0.01
Soil leachates										
Upland	Oi	i	6	9.0 ± 1.3	1.5 ± 0.8	2	437.1 ± 16.8	0.47 ± 0.00	1.02 ± 0.00	0.43 ± 0.00
		f	6	8.9 ± 1.3		1	446.2	0.51	1.00	0.43
	B	i	6	6.8 ± 1.0	2.0 ± 0.2	2	466.0 ± 40.6	0.57 ± 0.02	0.98 ± 0.02	0.42 ± 0.00
		f	6	6.7 ± 1.0		1	524.7	0.61	0.97	0.40

Table 1 (continued)

Catchment/position		i/f[a]	n for bulk	DOC (mg CL^{-1})	%BDOC	n for FT-ICR MS	Mass weighted average (Da)	O/C	H/C	AI_{mod}
Forested wetland	Oe	i	6	5.5 ± 0.4	Indistinguishable from 0	2	435.7 ± 7.8	0.49 ± 0.00	0.84 ± 0.00	0.55 ± 0.00
		f	6	5.5 ± 0.3		1	467.0	0.42	0.80	0.58
	Oa	i	6	6.8 ± 0.1	2.6 ± 1.6	2	450.8 ± 12.4	0.47 ± 0.01	0.88 ± 0.02	0.52 ± 0.01
		f	6	6.6 ± 0.2		1	473.5	0.42	0.74	0.61
	B	i	6	4.9 ± 0.2	3.7 ± 0.1	2	457.1 ± 29.7	0.49 ± 0.00	0.85 ± 0.02	0.53 ± 0.02
		f	6	4.7 ± 0.2		1	432.0	0.42	0.77	0.60
Fen	Oi	i	6	3.1 ± 0.2	Indistinguishable from 0	2	398.4 ± 16.3	0.48 ± 0.02	0.99 ± 0.07	0.45 ± 0.04
		f	6	3.2 ± 0.1		1	444.2	0.43	0.78	0.59
	Oe	i	6	6.4 ± 0.1	5.3 ± 1.0	2	456.1 ± 5.8	0.48 ± 0.01	0.88 ± 0.01	0.52 ± 0.01
		f	6	6.1 ± 0.1		1	459.8	0.39	0.80	0.59

[a]The symbol * denotes mean ± standard error DOC concentrations for all collected samples from individual trees for each tree DOM category, while i denotes the mean ± standard error DOC concentrations at the beginning of the incubation for the composite incubation sample. These initial timepoint samples are the ones for which BDOC and FT-ICR MS data are reported

[b]One of the DOC samples is a composite sample made of spruce stemflow samples from three different trees due to low volumes

[c]The three DOC samples are all composite samples made of hemlock stemflow samples from three different trees due to low volumes

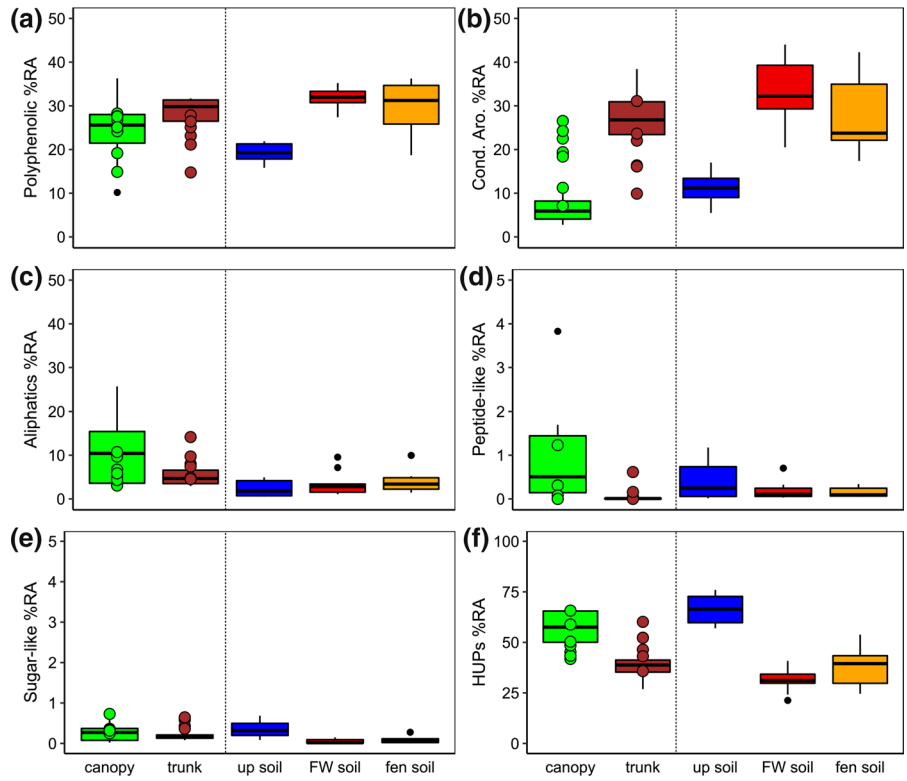

Fig. 3 Canopy (throughfall and needle leachates), trunk (stemflow and bark leachates), forested wetland (FW), fen, and upland FT-ICR MS compound classes. Throughfall and stemflow values are indicated by the colored points in the canopy and trunk categories; those boxes represent needle and bark leachate data. The median is represented by a horizontal line, boxes extend to the 25th and 75th percentiles, and whiskers extend to the minimum or maximum value or 1.5 times the interquartile range past the box (whichever is nearer the median). The black dots are outlying points past the whiskers' range

samples. Of the leachates, hemlock bark produced the most DOC (37.2 ± 5.5 mg CL^{-1}), while spruce bark produced the least (24.3 ± 4.2 mg CL^{-1}; Table 1). There was no significant difference between average hemlock and spruce leachate DOC concentrations ($p = 0.14$; Table S2). Soil leachate DOC concentration did not vary across the three landscape types ($p = 0.07$; Table 1 for concentrations; Table S3 for statistics).

There were no significant differences between spruce and hemlock when needle and bark leachate data or tree DOM samples for each species were combined for any FT-ICR MS compound classes or metrics for the initial sample timepoints. However, there were some significant differences between bark and needle leachates when including both species (Table S2). The mean H/C weighted average of the bark (0.88 ± 0.02) was significantly lower than that of the needles (1.08 ± 0.03; Fig. 2; $t_{10.4} = -5.11$, $p < 0.001$). Mean AI_{mod} weighted average was higher for bark than for needles (Fig. 2; 0.52 ± 0.01 vs. 0.39 ± 0.02; $t_{11.5} = 5.42$, $p < 0.001$). Heteroatom-containing formulae were more abundant in needles than bark; CHON ($t_{7.13} = -3.39$, $p < 0.05$) and CHOS ($t_{8.01} = -1.81$, $p = 0.11$) formulae made up 0.2 ± 0.1 and 1.4 ± 0.5%RA of bark and 3.1 ± 0.9 and 5.1 ± 2.0%RA of needle leachates, respectively (Table 2; Fig. S1). Bark contained relatively more condensed aromatics than did needles ($t_{9.62} = 8.31$, $p < 0.0001$; 28.5 ± 2.5 vs. 5.6 ± 1.1%RA; Fig. 3), and slightly but not significantly more polyphenolics ($t_{7.96} = 1.78$, $p = 0.11$; 29.2 ± 0.8 vs. 23.2 ± 3.2%RA; Fig. 3). Conversely, needles exceeded bark for peptide-like formulae ($t_{7.01} = -2.67$, $p < 0.05$; 1.2 ± 0.4 vs. 0.0 ± 0.0%RA; Fig. 3), and had slightly but not significantly higher aliphatic ($t_{7.98} = -1.36$, $p = 0.21$; 8.97 ± 2.8 vs. 5.0 ± 0.8%RA) and sugar-like ($t_{8.12} = -1.63$, $p = 0.14$; 0.3 ± 0.1 vs. 0.2 ± 0.0%RA) contributions.

Molecular compositions identified by FT-ICR MS were distinct in upland soil leachates compared to the combined wetland soil leachates. The upland soils had a smaller contribution of polyphenolics and condensed aromatics (19.0 ± 1.3 and 9.8 ± 2.0%RA; Table 2 for individual layers; Fig. 3) while they made up a greater contribution in the forested wetland and fen soils grouped together as wetland soils (30.4 ± 1.7 and 26.1 ± 1.8%RA respectively; Table 1

Table 2 FT-ICR MS compound and heteroatom classes for soil leachates, tree leachates, and tree DOM (stemflow and throughfall) initial (main sample) and final timepoints

Site		i/f	n	Cond. Aromatics (%RA)	Polyphenolics (%RA)	Aliphatics (%RA)	Sugar-like (%RA)	Peptide-like (%RA)	HUPs (%RA)	CHO (%RA)	CHON (%RA)	CHOS (%RA)	CHONS (%RA)
Tree stemflow and throughfall samples													
Rain			1	5.4	8.7	44.6	0.0	0.9	40.5	95.1	1.5	3.3	0.0
Spruce throughfall		i	2	18.7 ± 0.3	24.7 ± 0.5	6.3 ± 0.4	0.3 ± 0.0	0.0 ± 0.0	50.0 ± 0.3	99.2 ± 0.2	0.0 ± 0.0	0.8 ± 0.1	0.0 ± 0.0
		f	2	14.8 ± 7.7	20.9 ± 6.0	8.0 ± 2.8	0.4 ± 0.1	0.6 ± 0.6	55.5 ± 10.3	95.0 ± 0.8	1.7 ± 1.7	3.2 ± 0.9	0.1 ± 0.1
Spruce stemflow		i	2	13.0 ± 3.1	17.9 ± 3.2	11.9 ± 2.2	0.5 ± 0.1	0.4 ± 0.2	56.2 ± 4.0	94.7 ± 0.7	2.3 ± 1.0	2.4 ± 0.1	0.7 ± 0.2
		f	2	26.6 ± 4.5	25.5 ± 2.3	6.4 ± 1.6	0.3 ± 0.1	0.1 ± 0.0	41.1 ± 5.3	97.5 ± 0.7	0.5 ± 0.2	1.8 ± 0.6	0.1 ± 0.1
Hemlock throughfall		i	2	21.8 ± 2.4	27.6 ± 0.0	4.3 ± 0.0	0.3 ± 0.0	0.0 ± 0.0	45.9 ± 2.6	98.0 ± 1.3	0.4 ± 0.4	1.6 ± 0.9	0.0 ± 0.0
		f	2	18.9 ± 7.6	23.7 ± 4.5	6.4 ± 3.3	0.5 ± 0.2	0.2 ± 0.2	50.3 ± 8.5	96.3 ± 3.0	1.3 ± 1.3	2.2 ± 1.5	0.2 ± 0.2
Hemlock stemflow		i	2	20.0 ± 3.6	25.8 ± 0.7	6.0 ± 1.4	0.5 ± 0.1	0.1 ± 0.1	47.7 ± 4.6	96.7 ± 3.1	1.6 ± 1.6	1.7 ± 1.5	0.0 ± 0.0
Tree Leachates													
Epiphyte		i	2	11.6 ± 1.2	21.7 ± 0.2	6.4 ± 0.4	0.1 ± 0.0	0.1 ± 0.1	60.0 ± 2.0	98.0 ± 1.4	0.3 ± 0.3	1.7 ± 1.0	0.0 ± 0.0
		f	1	16.0	24.0	8.3	0.1	0.0	51.6	98.0	0.3	1.7	0.0
Spruce needles		i	4	4.5 ± 0.7	19.4 ± 4.5	11.9 ± 5.3	0.4 ± 0.1	1.9 ± 0.7	61.9 ± 3.0	87.3 ± 4.2	5.1 ± 0.7	7.6 ± 3.7	0.0 ± 0.0
		f	2	6.4 ± 1.2	26.9 ± 0.6	13.2 ± 3.2	0.2 ± 0.1	0.8 ± 0.6	52.6 ± 4.3	89.1 ± 0.4	2.4 ± 2.0	8.4 ± 2.5	0.0 ± 0.0
Spruce bark		i	4	26.6 ± 2.5	27.1 ± 0.7	6.8 ± 0.7	0.1 ± 0.0	0.0 ± 0.0	39.4 ± 2.5	97.3 ± 0.9	0.2 ± 0.1	2.4 ± 0.8	0.1 ± 0.1
		f	2	28.6 ± 2.1	25.7 ± 0.3	7.6 ± 0.6	0.3 ± 0.1	0.0 ± 0.0	37.9 ± 2.6	97.1 ± 0.9	0.3 ± 0.2	2.5 ± 1.2	0.0 ± 0.0
Hemlock needles		i	4	6.8 ± 2.1	27.0 ± 4.4	6.0 ± 1.8	0.1 ± 0.1	0.5 ± 0.2	59.6 ± 5.3	96.1 ± 1.0	1.1 ± 0.5	2.7 ± 0.5	0.1 ± 0.0
		f	2	10.6 ± 0.8	24.2 ± 0.7	18.0 ± 5.1	0.3 ± 0.3	0.1 ± 0.0	46.8 ± 3.9	86.5 ± 6.0	0.9 ± 0.4	12.6 ± 5.6	0.0 ± 0.0
Hemlock bark		i	4	30.5 ± 4.5	31.2 ± 0.2	3.2 ± 0.1	0.2 ± 0.0	0.0 ± 0.0	34.9 ± 4.6	99.2 ± 0.1	0.2 ± 0.1	0.5 ± 0.1	0.1 ± 0.1
		f	2	25.4 ± 1.7	31.4 ± 0.1	3.8 ± 0.1	0.2 ± 0.1	0.0 ± 0.0	39.1 ± 1.8	97.0 ± 2.2	0.1 ± 0.0	2.9 ± 2.2	0.1 ± 0.0
Soil endmembers													
Upland	Oi	i	2	15.3 ± 1.7	20.7 ± 1.1	4.8 ± 0.1	0.2 ± 0.1	1.0 ± 0.2	57.9 ± 1.0	89.2 ± 0.3	6.6 ± 0.2	3.9 ± 0.6	0.3 ± 0.2
		f	1	12.8	21.9	2.7	0.2	0.4	62.1	87.5	1.7	10.5	0.3
	B	i	2	9.2 ± 0.4	17.4 ± 1.5	0.8 ± 0.1	0.5 ± 0.2	0.1 ± 0.0	72.1 ± 1.3	91.4 ± 3.5	3.1 ± 0.3	4.8 ± 3.0	0.8 ± 0.2
		f	1	5.5	17.5	0.5	0.6	0.0	75.9	94.4	1.9	2.9	0.8
Forested wetland	Oe	i	2	32.8 ± 2.4	29.1 ± 1.8	2.4 ± 0.4	0.1 ± 0.0	0.2 ± 0.1	35.4 ± 1.1	92.3 ± 0.9	4.2 ± 0.2	2.8 ± 1.2	0.7 ± 0.2
		f	1	39.3	29.1	1.5	0.0	0.1	30.1	90.4	5.4	4.1	0
	Oa	i	2	28.0 ± 1.3	32.6 ± 0.7	8.4 ± 1.2	0.1 ± 0.0	0.5 ± 0.2	30.5 ± 0.7	86.5 ± 1.0	5.9 ± 1.4	7.0 ± 2.2	0.6 ± 0.3
		f	1	44.0	33.6	1.1	0.0	0.0	21.3	93.0	5.8	1.2	0.1
	B	i	2	26.4 ± 5.8	34.0 ± 1.2	3.2 ± 0.2	0.1 ± 0.1	0.1 ± 0.1	36.2 ± 4.6	90.7 ± 0.1	4.5 ± 1.8	4.5 ± 2.0	0.4 ± 0.4
		f	1	43.5	30.7	1.6	0.0	0.1	24.2	87.2	7.0	5.8	0.0
Fen	Oi	i	2	21.3 ± 3.9	21.7 ± 3.0	7.6 ± 2.4	0.2 ± 0.1	0.2 ± 0.1	49.1 ± 4.7	76.3 ± 13.9	3.55 ± 0.8	19.7 ± 14.9	0.4 ± 0.2

Table 2 (continued)

Site	i/f	n	Cond. Aromatics (%RA)	Polyphenolics (%RA)	Aliphatics (%RA)	Sugar-like (%RA)	Peptide-like (%RA)	HUPs (%RA)	CHO (%RA)	CHON (%RA)	CHOS (%RA)	CHONS (%RA)
	f	1	42.3	29.3	1.5	0.0	0.1	26.9	93.3	3.5	3.0	0.2
Oe	i	2	22.2 ± 0.1	34.7 ± 1.6	3.4 ± 0.4	0.1 ± 0.0	0.2 ± 0.1	39.5 ± 1.1	93.6 ± 0.8	0.5 ± 0.0	1.0 ± 0.2	0.4 ± 0.2
	f	1	38.2	35.2	2.0	0.0	0.1	24.6	92.7	0.6	2.2	0.1

for means by soil layer; significance levels for differences between watersheds in Table S3). Similarly, the upland soils had a lower mean AI_{mod} weighted average but greater mean H/C and O/C weighted averages than the wetlands lumped together (Fig. 2 for subcatchment values).

Tree and soil leachate BDOC and biodegradation driven shifts in DOM composition

Spruce stemflow had the highest BDOC of tree DOM samples (11.0 ± 1.0%), while minimal change was observed in spruce throughfall (0.8 ± 0.9%; Table 1; Fig. 2). No BDOC data were obtained from hemlock stemflow because of insufficient stemflow sample volume. Spruce stemflow had significantly greater BDOC than spruce and hemlock throughfall ($t_{6.00} = 3.46$, $p < 0.05$; Table S2 for statistics). Of the needle and bark leachate samples, spruce needles yielded the highest BDOC (56.0 ± 3.2%), while hemlock bark was the least bioavailable (10.4 ± 1.6%; Table 1). There was no significant difference between BDOC of spruce and hemlock leachates ($t_{41.1} = -1.79$, $p = 0.08$). Needle leachates had significantly higher BDOC than bark leachates ($t_{26.6} = -10.8$, $p < 0.001$). Percent BDOC was low in all soil leachate incubations, ranging from 5.3 ± 1.0% in fen O_e to no detectable decrease in both forested wetland O_e and fen O_i (Table 1). Soil leachate BDOC did not vary across the three landscape types ($p = 0.23$; Table 1 for percent BDOC; Table S3 for statistics).

A PCA of DOM composition for all tree leachates and tree DOM samples (and their final incubation time points) showed differences in DOM composition leached from different parts of the trees as well as some homogenization of DOM composition after biodegradation (Fig. 4a). On PC1, needles showed greater %RA of aliphatics, peptide-like, HUPs, and CHON- and CHOS-containing formulae, and lower %RA of condensed aromatics, polyphenolics, and CHO-containing formulae (Fig. 4b). Bark leachates clustered on the negative end of PC1. PC2 was dominated by %RA of sugar-like and CHONS-containing formulae, with needles separating slightly due to lower values and stemflow samples separating slightly due to greater relative abundances. The rain sample and epiphyte leachates grouped with the needles. No obvious separation by tree species occurred.

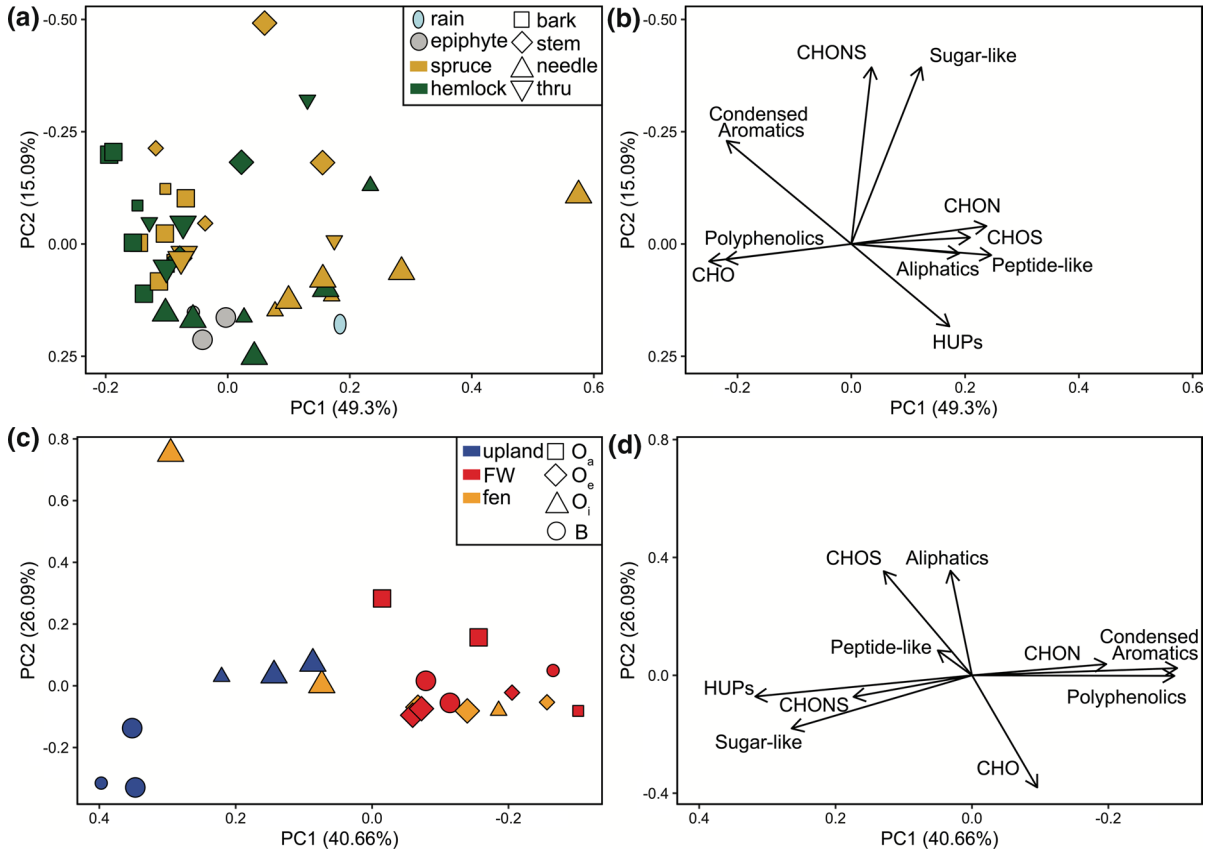

Fig. 4 **a**, **b** PCA of DOM composition for all tree leachates and stemflow and throughfall samples, along with their final incubation time points, to examine controls on aboveground tree DOM sources impacted by rainfall leaching. **c**, **d** PCA of DOM composition for both sets of soil leachates and soil leachate bioincubations to examine controls on belowground soil DOM sources impacted by both rainfall and groundwater leaching. **a/c** sample locations in PCA space and **b/d** loadings. Large symbols are initial incubation time points, small symbols are final incubation timepoints

A PCA of DOM composition for soil leachates and soil leachate bioincubations showed differences in DOM composition from soil leached from each sub-catchment and different directions of compositional change throughout the incubation in each sub-catchment (Fig. 4c). The upland soils separated from the wetland soils, and the final wetland time-points separated further from the initial wetland time-points. A greater %RA of condensed aromatics, polyphenolics, and CHON-containing formulae were most prevalent in final wetland soils while a greater %RA of HUPs, sugar-like and CHONS-containing formulae were indicative of upland soils (Fig. 4d).

Bioproduced formulae exceeded bioconsumed formulae in the fen and forested wetland (1193 vs. 670 and 738 vs. 132, respectively; Fig. 5). In contrast, there were fewer bioproduced than bioconsumed formulae in the upland site (181 vs. 265). Bioconsumed formulae in the upland had the highest AI_{mod} weighted average, while the forested wetland had the lowest (0.51 ± 0.01 and 0.18 ± 0.02). The opposite held true for bioproduced formulae, with the lowest AI_{mod} weighted average in the upland and highest in forested wetland (0.43 ± 0.01 and 0.69 ± 0.00, respectively). The upland had the lowest mean H/C and O/C weighted averages for bioconsumed formulae and the highest for bioproduced formulae (0.90 ± 0.02, 0.38 ± 0.01, 0.93 ± 0.02, and 0.54 ± 0.01, respectively), while the forested wetland had the highest for bioconsumed formulae and the lowest H/C for bioproduced formulae (1.39 ± 0.03, 0.56 ± 0.02, and 0.62 ± 0.01).

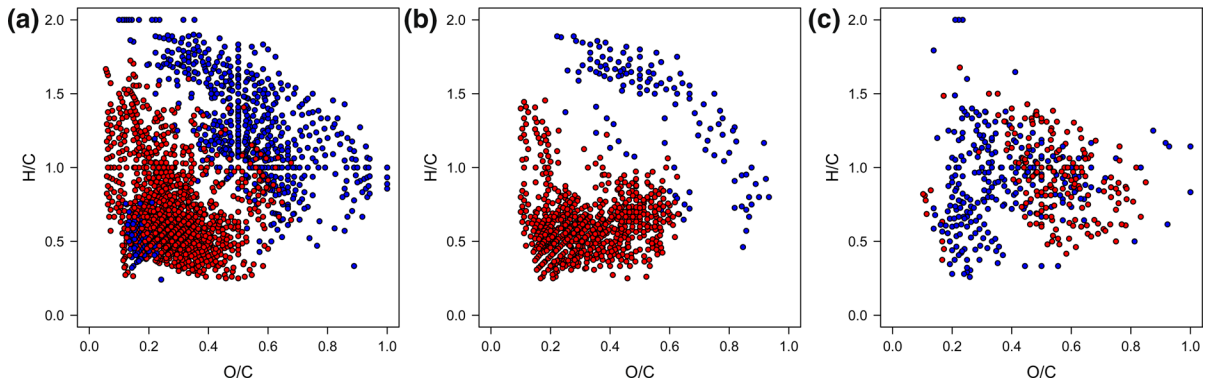

Fig. 5 Formulae either bioconsumed (blue) or bioproduced (red) in all soil incubations for the **a** fen, **b** forested wetland, and **c** upland

Table 3 Number of unique molecular formulae present in all samples from one DOM source and in no samples from any other DOM sources. Number and percent of those unique molecular formulae that were completely bioconsumed during bioincubations (- represents no unique formulae at the start of incubations)

Tree DOM source	# unique in all	# (%) bio-consumed
Spruce needle	0	–
Spruce throughfall	0	–
Spruce bark	1	0 (0)
Spruce stemflow	176	162 (92)
Hemlock needle	0	–
Hemlock throughfall	1	1 (100)
Hemlock bark	0	–
Hemlock stemflow	0	–
Epiphytes	11	9 (82)
Fen Oi	1	1 (100)
Fen Oe	4	3 (75)
Forested wetland Oe	0	–
Forested wetland Oa	20	12 (60)
Forested wetland B	1	1 (100)
Upland Oi	36	36 (100)
Upland B	1	1 (100)

The fen had the lowest bioproduced O/C weighted average (0.28 ± 0.00).

Biodegradation reduces source-specific marker formulae

Unique formulae (present in all samples from one DOM source and in no samples from any other DOM source) were identified in less than half of the tree leachates or tree DOM samples and all but one soil leachate (Table 3; Table S4 for unique formulae list). Most sources had fewer than five unique formulae, while spruce stemflow had 176 unique formulae identified. Of the unique formulae, nearly all formulae (90%) were bioconsumed in all samples over the course of the 14-day incubations. Unique formulae in hemlock throughfall, fen O_i, forested wetland B, upland O_i, and upland B leachates were completely consumed.

Discussion

Soil wetness drives DOM composition and microbial processing

Leachable DOM in wetland soils was more aromatic than in upland soils, as supported by the greater contributions of condensed aromatics and polyphenolics and higher AI_{mod} in wetland soils (Figs. 2 and 3; Tables 1 and 2). Phenolic compounds have long been associated with organic matter preservation in wetland soils where anaerobic conditions limit phenolic oxidation (Freeman et al. 2001; Limpens et al. 2008). These findings suggest that phenolic compound breakdown was likely inhibited in the saturated wetland soils while enhanced in the well aerated upland soils.

Antecedent soil saturation and associated anaerobic conditions appear to be a primary control on soil leachate DOM composition and drive a divergence

in composition between wetland and upland sites during bioincubations (Fig. 4c, d). Each soil layer progressed along PC1 from the initial to final time point with the direction of movement depending on the type of soil (wetland and upland layers moving farther apart). DOM leached from wetland soils had high consumption of high H/C, aliphatic, sugar-like, and peptide-like formulae (Fig. 5; Tables 1 and 2), which were likely targets for microbial degradation since high H/C ratio-formulae have greater stored energy (Hopkinson et al. 1998; Smith et al. 2018; Textor et al. 2019). When the soil layers were leached and incubated in the laboratory, soil microbes were likely exposed to more aerobic conditions than were originally present in situ. Thus, it is possible that aerobic incubation lifted the anoxic hold on the biolabile, energy-rich compounds that microbes could consume, increasing the relative abundance of aromatic DOM remaining following incubation. During periods of abundant precipitation, NPCTR soils become saturated and anerobic, while during dry periods in spring and early summer, water table drawdown leads to deeper soil aerobic zones (D'Amore et al. 2015b; Emili and Price 2013). Therefore, our leaching methods may partially mimic the regular fluctuations in water table height previously observed in the wetland sites (D'amore et al. 2010).

The opposite trend in DOM composition following laboratory incubations was observed in the upland leachates. Microbial processing decreased the %RA of condensed aromatics (Antony et al. 2017; Bandowe et al. 2019), and a number of condensed aromatic formulae were completely consumed (Fig. 5). Bioproduced formulae were mainly located in the center of H/C versus O/C space. The same pattern of more centralized formulae in H/C versus O/C space was previously seen in DOM with increasing soil depth (Roth et al. 2019), contracting into the HUPs region which increased its %RA in this study's upland soil leachates (unlike in the wetland leachates). This convergence in the center of van Krevelen space of DOM molecular composition is common during microbial processing (Behnke et al. 2021; Kellerman et al. 2018; Roth et al. 2019). Since upland soils in the NPCTR are usually unsaturated (D'Amore et al. 2015a), it is likely no dramatic reoxygenation took place during leaching. Biolabile DOM is consumed in situ by microbial communities as it is produced, preventing the accumulation of specific DOM compound classes as observed in the wetland sites.

These compositional shifts during bioincubation occur despite overall low bioavailability of soil leachate DOC (1.5–5.3% or <0.5 mg CL^{-1}; Table 1). Some otherwise biodegradable DOC may have been lost or modified during the drying process prior to leaching, partially explaining these low BDOC values. However our values are generally consistent with previous soil and peatland BDOC trends in the NPCTR and elsewhere (Fellman et al. 2017; Hansen et al. 2016; Payandi-Rolland et al. 2020; Shirokova et al. 2019). Our findings thus support the idea that microbial degradation of DOM leached from soils can shift DOM composition even with marginal decreases in DOC concentration ($<10\%$; Hansen et al. 2016).

Tree DOC in the NPCTR

To our knowledge, these are the first reported throughfall or stemflow DOC concentrations for the northern NPCTR. Stemflow samples had higher average DOC concentrations than throughfall (Fig. 2a) as previously reported in both coniferous (Thieme et al. 2019) and deciduous (Howard et al. 2018; Van Stan et al. 2017) temperate forests. This is likely because stemflow has longer residence time in contact with the tree trunk and thus greater opportunity to leach organic material.

Our mean hemlock and spruce throughfall and stemflow values (Table 1) were greater than almost all reported throughfall (median: 11 mg CL^{-1}) and stemflow (median: 22 mg CL^{-1}) values from a global review of different forest tree DOM characteristics (Van Stan and Stubbins 2018). These high DOC concentrations are not surprising due to the large surface area of spruce and hemlock needles and the trees' multilayered bark. Lower canopy-wide throughfall DOC values of 19.8 ± 10.8 mg CL^{-1} have been reported for the Southern NPCTR where the forest is dominated by a different mix of conifer species (Emili and Price 2013). The lower contribution of Sitka spruce in the Southern NPCTR may explain the lower DOC concentrations, given spruce's consistently higher DOC concentrations found in this study, though the concentration differences could also be due to variations in canopy coverage of trees sampled. Though stemflow and throughfall volume were not systematically assessed for this study,

hemlock throughfall reached > 3.4 cm deep and a single spruce's stemflow exceeded 600 mL for one two-day storm event (data not shown). We hypothesize that because of the abundant regional precipitation (Lader et al. 2020), resulting in high stemflow and throughfall volumes, and the high DOC concentrations reported here, there is potential for large mobilization of tree DOM during storm events which may contribute to watershed carbon export if not mineralized or stabilized in soils before delivery to surface waters. These results highlight the importance of measuring regional stemflow and throughfall fluxes and including tree sources in future studies that investigate the origins of DOM in forested watersheds.

DOM compositional differences between bark and needles

Dramatic compositional differences between needle and bark leachates demonstrate more variation between individual tree canopies and trunks than between species. Needle leachates were compositionally unique, with the majority clustering together in the PCA (featuring high peptide-like, aliphatic, and N- and S- contribution) while bark leachates, stemflow, and throughfall intermingled, suggesting the stronger resemblance of natural tree DOM to bark leachates than to needle leachates (Fig. 4a-b). Saturation of needles and tree trunks occurs during large rain events, but the processes of leaching in the laboratory may more closely resemble fallen needles or bark in standing water on the forest floor. The similarity of the composition of hemlock and spruce leachates (both for bark and for needles) likely stems from the species' close evolutionary relationship and makes molecular source attribution of DOM to a specific species challenging. *Tsuga* species and *Picea* species are part of adjacent clades in the Pinaceae family (Gernandt et al. 2018). This presumably explains their molecular similarity compared to other pairs of trees whose tree DOM has been studied in the past which belonged to different families and whose molecular differentiation corresponded with their phylogenetic separation (Stubbins et al. 2017; Van Stan et al. 2017).

Aromatic and high molecular weight formulae enrichment in oak stemflow versus throughflow has been attributed to greater contact with bark and canopy soils (Stubbins et al. 2017), since bark microtopography can increase water-bark contact time and the potential for leaching aromatic DOM (Levia et al. 2012). The aromatic stemflow and throughfall in this study (mean AI_{mod} for tree DOM ranging from 0.39 to 0.49) suggests rainfall intercepting spruce and hemlock trees has substantial bark interaction, possibly due to the conifers' thin needles directing throughfall over small bark covered twigs.

A vegetation source of condensed aromatics

In this study, formulae termed condensed aromatics based on certain basic assumptions about DOM chemistry and stoichiometry (Koch and Dittmar 2006, 2016) contributed as much as 38.4%RA to tree bark leachate DOM (Fig. 3b). Condensed aromatics also contribute substantially to wetland leachate and tree DOM. These tree DOM condensed aromatic values were up to four times higher than those previously reported in Southeast Alaskan streams, though use of different FT-ICR MS instruments complicate direct comparison due to individual instrument settings (< 10%; Behnke et al. 2020; Fellman et al. 2020; Holt et al. 2021), and substantially exceeded condensed aromatics in a global riverine DOM survey analyzed on the same instrument used in this study (< 20%; Kellerman et al. 2018).

Condensed aromatic formulae are often thermogenic and are regularly associated with fossil fuel or biomass burning (Dittmar and Koch 2006; Koch and Dittmar 2006; Kramer et al. 2004). Their presence in ecosystems has been used as a marker of combustion byproducts such as soot aerosols (Spencer et al. 2014; Stubbins et al. 2012), and their presence in stemflow and throughfall has previously been attributed to rainfall washing deposition products off trees (Stubbins et al. 2017; Van Stan and Stubbins 2018). Combustion byproducts are widely deposited even in remote regions and have long potential lifetimes in the atmosphere (Khan et al. 2016; Ogren and Charlson 1983; Xu et al. 2009). Pollutants can accumulate on both leaves and bark of trees via dry deposition (Schulz et al. 1999; Xu et al. 2018). Therefore, it is possible that tree bark in Southeast Alaska (which stays on trees longer than needles) serves as a long-term integrator of deposited combustion byproducts.

However, bark leachates of both species studied here had far higher condensed aromatic contribution than did needle leachates. Tree canopies have been

shown to limit atmospheric deposition on surfaces underneath them (Liu et al. 2007), suggesting that bark under the thick evergreen canopy are less likely to receive deposition than are the canopies themselves. Given the extensive and year-round canopy cover of spruce and hemlock trees, it appears unlikely that anthropogenic combustion byproducts could be deposited in such great abundance on tree bark and yet leave needles (the first interception point between tree and sky) so unaffected. Fire is rare in the coastal temperate rainforest of Southeast Alaska, with fire return intervals on the scale of thousands of years (Lertzman et al. 2002), so regional biomass burning is an unlikely condensed aromatic source.

Recently, multiple studies have identified the probability of non-combustion based (Wagner et al. 2019a) and terrestrial sources of condensed aromatics, with increasing condensed aromatic contribution corresponding to allochthonous, terrestrial inputs (DiDonato et al. 2016; Johnston et al. 2020; Kellerman et al. 2018) including in Southeast Alaska (Behnke et al. 2020; Holt et al. 2021). Our findings suggest a conifer bark source of condensed aromatics may supplement the background depositional sources present in the study site. Bark microrelief increases water-bark interactions, leaching, and production of aromatic hydrocarbons and highly aromatic DOM (Levia et al. 2012), and fungi inhabit the crevasses and inner bark of trees (Magyar 2008; Tejesvi et al. 2005). Some fungi produce ligninolytic enzymes that can degrade lignin through radical intermediates (Higuchi 2004). Hydroxyl radicals (which can be generated by a variety of processes) have in turn been shown to produce condensed aromatic formulae from lignin through decarboxylation and condensation (Waggoner et al. 2015; Waggoner and Hatcher 2017). Further, fungi are capable of biosynthesizing condensed aromatic cores through enzyme-mediated cyclization and condensation (Gao et al. 2016). Though the mechanism has not been tested here and should be the subject of future study, we think it possible that fungal mediated lignin degradation occurring within bark crevasses may lead to the formation of condensed aromatic formulae through pathways similar to those previously observed (Waggoner et al. 2015; Waggoner and Hatcher 2017), particularly since biological processes have already been suggested to form condensed aromatics (Chen et al. 1998; Daisy et al. 2002). This terrestrial source may then be preserved in the wetland soils either due to leaching from bark decaying on the forest floor, or due to transport and retention of condensed aromatic formulae via water from trees to soil.

Microbial degradation homogenizes tree DOM sources and resolves soil DOM sources

In this study, DOM from diverse tree sources became more similar with microbial processing (Fig. 4a), as observed during the microbial buffering and compositional convergence previously proposed to decrease the diversity of plant leachate DOM (Harfmann et al. 2019; Hensgens et al. 2021). This contrasts with the soil leachate final time points, which progress towards the outside of PC1, separating from the initial time points as microbially degraded soil DOM became more diverse (Fig. 4c). The high biolability of the tree DOM incubations in this study may in part explain their compositional stability. Since all compound classes present in tree DOM samples are at least moderately bioavailable in at least one tree DOM sample, the uniform degradation of different yet all bioavailable compound classes throughout the tree DOM dataset appears to have not provided the uniform compositional shift often associated with microbial degradation of soil DOM (Hansen et al. 2016; Textor et al. 2019).

Microbial buffering and compositional convergence do not appear to hold true for the soil leachates, even at the bulk level. Initial soil wetness dictated the greater separation of final than initial soil leachates on PC1 (Fig. 4c). Therefore, though most of the marker molecular formulae from specific soil layer sources disappear during microbial degradation, the fundamental separation between DOM sourced from wetland soils versus upland soils strengthens. Though exact watershed residence time is not known, the 14-day bioincubations are substantially longer than the hours to a few days response time of the sub-catchments to changes in precipitation (Fellman et al. 2009b, 2020). These findings suggest that the source-specific marker formulae that persisted throughout the incubation are conservative; those and possibly more of the source-specific formulae are likely to remain unmodified through the watershed's flow network. How well this reflects in situ processing of soil DOM by microbes upon natural leaching remains to

be seen, but the concept of source convergence and homogenization via microbial buffering (Harfmann et al. 2019) appears limited to freshly leached plant inputs.

Future implications for terrestrial DOM sources in the NPCTR

Climate change in the NPCTR is predicted to alter carbon storage and decomposition rates along with hydroclimatology as warming is projected to shift the dominant form of precipitation from snow to rain in winter (Bidlack et al. 2021; McAfee et al. 2014). Decreasing annual snowpack causes smaller and earlier snowmelt pulses, leading to lower flows in late summer and early fall (Shanley et al. 2015) and a possible increase in summer drought events (Lader et al. 2020; Mote and Salathé 2010). Warming-induced drought enhancement combined with high rates of evapotranspiration in spring and early summer could lead to increasing water table drawdown and expanding aerobic zones for DOM processing in soils (D'amore et al. 2010, 2015a; Emili and Price 2013). Further, the predicted increase in high intensity rain events in the region (Lader et al. 2020) has the potential to increase the flux of tree DOM to forest floors. Storm events have the ability to shunt terrestrially sourced DOM further downstream than under baseflow conditions by bypassing microbial degradation along the terrestrial-aquatic continuum (Raymond et al. 2016; Wagner et al. 2019b). It is thus possible that intensifying hydroclimatic regimes in the NPCTR will lead to more highly bioavailable and less degraded DOM (including more source-specific molecular formulae) being exported to coastal oceans during storm events, moving the location of DOM processing towards the ocean.

Conclusions

We have documented the unique molecular signatures and characteristics of DOM sources in the Northern NPCTR, and uncovered the following trends:

(1) The soil saturation gradient dictates initial DOM composition of soil leachates and the compositional shift that DOM undergoes during microbial processing.
(2) Differences between DOM produced from the canopy and trunk of a given tree are greater than differences between species. Tree DOC flux may be substantial and needs to be quantified.
(3) Coniferous trees in the NPCTR may be a previously unrecognized source of condensed aromatic formulae to DOM (possibly via fungal mediated lignin degradation). These could be transported to surface waters and exported from catchments.
(4) Biodegradation removes unique marker formulae of individual source leachates but retains bulk source DOM characteristics. In soils, biodegradation leads to a divergence rather than a convergence of soil DOM composition in contrast to the homogenizing effect of biodegradation on plant leachate DOM.

Acknowledgements The authors thank Emily Whitney for her invaluable field, laboratory, and logistical assistance and Molly Tankersley for creating Fig. 1. They are also grateful to all the helpful researchers at the National High Magnetic Field Laboratory who enabled data acquisition and processing. This work took place on the lands of the Aak'w Kwáan Tlingit.

Author contributions The study was conceived and designed by MIB, JBF, DVD, and RGMS. Sample collection and experimentation were performed by MIB, JBF, and DVD. Sample processing and analysis were performed by MIB and SMG. The first draft of the manuscript was written by MIB and all authors commented on previous versions of the manuscript. All authors read and approved the final manuscript.

Funding This work was supported by the National Science Foundation through an NSF Graduate Research Fellowship to MIB. A portion of this work was performed at the National High Magnetic Field Laboratory ICR User Facility, which is supported by the National Science Foundation Division of Chemistry and Division of Materials Research through DMR-1644779 and the State of Florida. Conflicts of interest/Competing interests: The authors have no conflicts of interests to declare.

Data availability All FT-ICR MS and DOC data are freely available on the Open Science Framework (https://osf.io/4azm8/; https://doi.org/10.17605/OSF.IO/BRJWC).

Code availability Not applicable.

Declarations

Conflict of interest The authors have not disclosed any competing interests.

References

Antony R, Willoughby AS, Grannas AM et al (2017) Molecular insights on dissolved organic matter transformation by supraglacial microbial communities. Environ Sci Technol 51:4328–4337. https://doi.org/10.1021/acs.est.6b05780

Bandowe BAM, Leimer S, Meusel H et al (2019) Plant diversity enhances the natural attenuation of polycyclic aromatic compounds (PAHs and oxygenated PAHs) in grassland soils. Soil Biol Biochem 129:60–70. https://doi.org/10.1016/j.soilbio.2018.10.017

Behnke M, Stubbins A, Fellman JB, Hood E, Dittmar T, Spencer RGM (2020) Dissolved organic matter sources in glacierized watersheds delineated through compositional and carbon isotopic modeling. Limnol Oceanogr. https://doi.org/10.1002/lno.11615

Behnke M, McClelland J, Tank S et al (2021) Pan-Arctic riverine dissolved organic matter: synchronous molecular stability, shifting sources and subsidies. Glob Biogeochem Cycles. https://doi.org/10.1029/2020GB006871

Bidlack AL, Bisbing SM, Buma BJ et al (2021) Climate-mediated changes to linked terrestrial and marine ecosystems across the northeast Pacific coastal temperate rainforest margin. Bioscience. https://doi.org/10.1093/biosci/biaa171

Buma B, Krapek J, Edwards RT (2016) Watershed-scale forest biomass distribution in a perhumid temperate rainforest as driven by topographic, soil, and disturbance variables. Can J for Res 46:844–854. https://doi.org/10.1139/cjfr-2016-0041

Chen J, Henderson G, Grimm C, Lloyd S, Laine R (1998) Termites fumigate their nests with naphthalene. Nature 392:558. https://doi.org/10.1038/33305

Corilo Y (2015) PetroOrg. Florida State University

D'amore DV, Fellman JB, Edwards RT, Hood E (2010) Controls on dissolved organic matter concentrations in soils and streams from a forested wetland and sloping bog in southeast Alaska. Ecohydrology 3:249–261. https://doi.org/10.1002/eco.101

D'Amore DV, Fellman JB, Edwards RT, Hood E, Ping C-L (2012) Hydropedology of the North American coastal temperate rainforest. Hydropedology. https://doi.org/10.1016/B978-0-12-386941-8.00011-3

D'Amore DV, Edwards RT, Herendeen PA, Hood E, Fellman JB (2015a) Dissolved organic carbon fluxes from hydropedologic units in Alaskan coastal temperate rainforest watersheds. Soil Sci Soc Am J 79:378–388. https://doi.org/10.2136/sssaj2014.09.0380

D'Amore DV, Ping C-L, Herendeen PA (2015b) Hydromorphic soil development in the coastal temperate rainforest of Alaska. Soil Sci Soc Am J 79:698–709. https://doi.org/10.2136/sssaj2014.08.0322

Daisy BH, Strobel GA, Castillo U, Ezra D, Sears J, Weaver DK, Runyon JB (2002) Naphthalene, an insect repellent, is produced by *Muscodor vitigenus*, a novel endophytic fungus. Microbiology 148:3737–3741. https://doi.org/10.1099/00221287-148-11-3737

DiDonato N, Chen H, Waggoner D, Hatcher PG (2016) Potential origin and formation for molecular components of humic acids in soils. Geochim Cosmochim Acta 178:210–222. https://doi.org/10.1016/j.gca.2016.01.013

Dittmar T, Koch BP (2006) Thermogenic organic matter dissolved in the abyssal ocean. Mar Chem 102:208–217. https://doi.org/10.1016/j.marchem.2006.04.003

Dittmar T, Koch B, Hertkorn N, Kattner G (2008) A simple and efficient method for the solid-phase extraction of dissolved organic matter (SPE-DOM) from seawater. Limnol Oceanogr: Methods 6:230–235. https://doi.org/10.4319/lom.2008.6.230

Edwards RT, D'Amore DV, Biles FE, Fellman JB, Hood EW, Trubilowicz JW, Floyd WC (2021) Riverine dissolved organic carbon and freshwater export in the eastern Gulf of Alaska. J Geophys Res: Biogeosci 126:5725. https://doi.org/10.1029/2020JG005725

Emili LA, Price JS (2013) Biogeochemical processes in the soil-groundwater system of a forest-peatland complex, north coast British Columbia, Canada. Northwest Sci 87:326–348. https://doi.org/10.3955/046.087.0406

Fellman JB, D'Amore DV, Hood E, Boone RD (2008) Fluorescence characteristics and biodegradability of dissolved organic matter in forest and wetland soils from coastal temperate watersheds in southeast Alaska. Biogeochemistry 88:169–184. https://doi.org/10.1007/s10533-008-9203-x

Fellman JB, Hood E, D'Amore DV, Edwards RT, White D (2009a) Seasonal changes in the chemical quality and biodegradability of dissolved organic matter exported from soils to streams in coastal temperate rainforest watersheds. Biogeochemistry 95:277–293

Fellman JB, Hood E, Edwards RT, D'Amore DV (2009b) Changes in the concentration, biodegradability, and fluorescent properties of dissolved organic matter during stormflows in coastal temperate watersheds. J Geophys Res: Biogeosci 114:G01021. https://doi.org/10.1029/2008JG000790

Fellman JB, D'Amore DV, Hood E, Cunningham P (2017) Vulnerability of wetland soil carbon stocks to climate warming in the perhumid coastal temperate rainforest. Biogeochemistry 133:165–179. https://doi.org/10.1007/s10533-017-0324-y

Fellman JB, Hood E, Behnke MI, Welker JM, Spencer RG (2020) Stormflows drive stream carbon concentration, speciation and dissolved organic matter composition in coastal temperate rainforest watersheds. Biogeosci, J Geophys Res. https://doi.org/10.1029/2020JG005804

Freeman C, Ostle N, Kang H (2001) An enzymic'latch'on a global carbon store. Nature 409:149. https://doi.org/10.1038/35051650

Gao S-S, Duan A, Xu W, Yu P, Hang L, Houk K, Tang Y (2016) Phenalenone polyketide cyclization catalyzed by fungal polyketide synthase and flavin-dependent monooxygenase. J Am Chem Soc 138:4249–4259. https://doi.org/10.1021/jacs.6b01528

Gernandt DS, Reséndiz Arias C, Terrazas T, Aguirre Dugua X, Willyard A (2018) Incorporating fossils into the Pinaceae tree of life. Am J Bot 105:1329–1344. https://doi.org/10.1002/ajb2.1139

Groeneveld M, Tranvik L, Natchimuthu S, Koehler B (2016) Photochemical mineralisation in a boreal brown water

lake: considerable temporal variability and minor contribution to carbon dioxide production. Biogeosciences 13:3931–3943. https://doi.org/10.5194/bg-13-3931-2016

Guggenberger G, Zech W, Schulten H-R (1994) Formation and mobilization pathways of dissolved organic matter: evidence from chemical structural studies of organic matter fractions in acid forest floor solutions. Org Geochem 21:51–66. https://doi.org/10.1016/0146-6380(94)90087-6

Hansen AM, Kraus TE, Pellerin BA, Fleck JA, Downing BD, Bergamaschi BA (2016) Optical properties of dissolved organic matter (DOM): Effects of biological and photolytic degradation. Limnol Oceanogr 61:1015–1032. https://doi.org/10.1002/lno.10270

Harfmann JL, Guillemette F, Kaiser K, Spencer RG, Chuang CY, Hernes PJ (2019) Convergence of terrestrial dissolved organic matter composition and the role of microbial buffering in aquatic ecosystems. J Geophys Res: Biogeosci 124:3125–3142. https://doi.org/10.1029/2018JG004997

Heath LS, Smith JE, Woodall CW, Azuma DL, Waddell KL (2011) Carbon stocks on forestland of the United States, with emphasis on USDA Forest Service ownership. Ecosphere 2:1–21. https://doi.org/10.1890/ES10-00126.1

Hensgens G, Lechtenfeld OJ, Guillemette F, Laudon H, Berggren M (2021) Impacts of litter decay on organic leachate composition and reactivity. Biogeochemistry. https://doi.org/10.1007/s10533-021-00799-3

Hertkorn N, Ruecker C, Meringer M et al (2007) High-precision frequency measurements: indispensable tools at the core of the molecular-level analysis of complex systems. Anal Bioanal Chem 389:1311–1327. https://doi.org/10.1007/s00216-007-1577-4

Higuchi T (2004) Microbial degradation of lignin: role of lignin peroxidase, manganese peroxidase, and laccase. Proc Jpn Acad Ser B 80:204–214. https://doi.org/10.2183/pjab.80.204

Holt AD, Fellman J, Hood E et al (2021) The evolution of stream dissolved organic matter composition following glacier retreat in coastal watersheds of southeast Alaska. Biogeochemistry. https://doi.org/10.1007/s10533-021-00815-6

Hopkinson CS, Buffam I, Hobbie J et al (1998) Terrestrial inputs of organic matter to coastal ecosystems: an intercomparison of chemical characteristics and bioavailability. Biogeochemistry 43:211–234. https://doi.org/10.1023/A:1006016030299

Horikoshi M, Tang Y (2016) ggfortify: Data visualization tools for statistical analysis results. See https://CRANR-project.org/package=ggfortify

Howard DH, VanStan JT, Whitetree A, Zhu L, Stubbins A (2018) Interstorm variability in the biolability of tree-derived dissolved organic matter (tree-DOM) in throughfall and stemflow. Forests 9:236. https://doi.org/10.3390/f9050236

Inamdar S, Finger N, Singh S et al (2012) Dissolved organic matter (DOM) concentration and quality in a forested mid-Atlantic watershed, USA. Biogeochemistry 108:55–76. https://doi.org/10.1007/s10533-011-9572-4

Johnston SE, Bogard MJ, Rogers JA, Butman D, Striegl RG, Dornblaser M, Spencer RG (2019) Constraining dissolved organic matter sources and temporal variability in a model sub-Arctic lake. Biogeochemistry 146:271–292. https://doi.org/10.1007/s10533-019-00619-9

Johnston SE, Striegl RG, Bogard MJ et al (2020) Hydrologic connectivity determines dissolved organic matter biogeochemistry in northern high-latitude lakes. Limnol Oceanogr 65:1764–1780. https://doi.org/10.1002/lno.11417

Kaiser NK, Quinn JP, Blakney GT, Hendrickson CL, Marshall AG (2011) A novel 9.4 Tesla FTICR mass spectrometer with improved sensitivity, mass resolution, and mass range. J Am Soc Mass Spectrom 22:1343–1351. https://doi.org/10.1007/s13361-011-0141-9

Kassambara A (2020) rstatix: pipe-friendly framework for basic statistical tests

Keith H, Mackey BG, Lindenmayer DB (2009) Re-evaluation of forest biomass carbon stocks and lessons from the world's most carbon-dense forests. Proc Natl Acad Sci USA 106:11635–11640. https://doi.org/10.1073/pnas.0901970106

Kellerman AM, Fo G, Podgorski DC, Aiken GR, Butler KD, Spencer RG (2018) Unifying concepts linking dissolved organic matter composition to persistence in aquatic ecosystems. Environ Sci Technol 52:2538–2548. https://doi.org/10.1021/acs.est.7b05513

Khan AL, Jaffé R, Ding Y, McKnight DM (2016) Dissolved black carbon in Antarctic lakes: chemical signatures of past and present sources. Geophys Res Lett 43:5750–5757. https://doi.org/10.1002/2016GL068609

Koch B, Dittmar T (2006) From mass to structure: an aromaticity index for high-resolution mass data of natural organic matter. Rapid Commun Mass Spectrom 20:926–932. https://doi.org/10.1002/rcm.2386

Koch B, Dittmar T, Witt M, Kattner G (2007) Fundamentals of molecular formula assignment to ultrahigh resolution mass data of natural organic matter. Anal Chem 79:1758–1763. https://doi.org/10.1021/ac061949s

Koch B, Dittmar T (2016) From mass to structure: an aromaticity index for high-resolution mass data of natural organic matter. Rapid Commun Mass Spectrom 20:926–932. https://doi.org/10.1002/rcm.7433

Koehler B, Landelius T, Weyhenmeyer GA, Machida N, Tranvik LJ (2014) Sunlight-induced carbon dioxide emissions from inland waters. Glob Biogeochem Cycles 28:696–711. https://doi.org/10.1002/2014GB004850

Kramer RW, Kujawinski EB, Hatcher PG (2004) Identification of black carbon derived structures in a volcanic ash soil humic acid by Fourier transform ion cyclotron resonance mass spectrometry. Environ Sci Technol 38:3387–3395. https://doi.org/10.1021/es030124m

Kurek MR, Stubbins A, Drake TW et al (2021) Drivers of organic molecular signatures in the Amazon River. Glob Biogeochem Cycles. https://doi.org/10.1029/2021GB006938

Lader R, Bidlack A, Walsh JE, Bhatt US, Bieniek PA (2020) Dynamical downscaling for Southeast Alaska: historical climate and future projections. J Appl Meteorol Climatol. https://doi.org/10.1175/JAMC-D-20-0076.1

Lertzman K, Gavin D, Hallett D, Brubaker L, Lepofsky D, Mathewes R (2002) Long-term fire regime estimated from soil charcoal in coastal temperate rainforests. Conserv Ecol. https://doi.org/10.5751/es-00432-060205

Levia DF, Van Stan I, John T, Inamdar SP et al (2012) Stemflow and dissolved organic carbon cycling: temporal variability in concentration, flux, and UV-Vis spectral metrics in a temperate broadleaved deciduous forest in the eastern United States. Can J for Res 42:207–216. https://doi.org/10.1139/X11-173

Limpens J, Berendse F, Blodau C et al (2008) Peatlands and the carbon cycle: from local processes to global implications: a synthesis. Biogeosciences 5:1475–1491. https://doi.org/10.5194/bg-5-1475-2008

Liu X-Y, Xiao H-Y, Liu C-Q, Li Y-Y (2007) $\delta^{13}C$ and $\delta^{15}N$ of moss *Haplocladium microphyllum* (Hedw.) Broth. for indicating growing environment variation and canopy retention on atmospheric nitrogen deposition. Atmos Environ 41:4897–4907. https://doi.org/10.1016/j.atmosenv.2007.02.004

Magyar D (2008) The tree bark: a natural spore trap. Asp Appl Biol 89:7–16

McAfee SA, Walsh J, Rupp TS (2014) Statistically downscaled projections of snow/rain partitioning for Alaska. Hydrol Processes 28:3930–3946. https://doi.org/10.1002/hyp.9934

McNicol G, Bulmer C, D'Amore D et al (2019) Large, climate-sensitive soil carbon stocks mapped with pedology-informed machine learning in the North Pacific coastal temperate rainforest. Environ Res Lett 14:014004. https://doi.org/10.1088/1748-9326/aaed52

Mote PW, Salathé EP (2010) Future climate in the Pacific Northwest. Clim Change 102:29–50. https://doi.org/10.1007/s10584-010-9848-z

Nash D, Waliser D, Guan B, Ye H, Ralph FM (2018) The role of atmospheric rivers in extratropical and polar hydroclimate. J Geophys Res Atmos 123:6804–6821. https://doi.org/10.1029/2017JD028130

National Wetlands Working Group (1988) Wetlands of Canada. Ecological land classification series, no. 24. Sustainable Development Branch, Environment Canada, Ottawa, Ontario, and Polyscience Publications Inc, Montreal, Quebec

Ogren J, Charlson R (1983) Elemental carbon in the atmosphere: cycle and lifetime. Tellus B 35:241–254. https://doi.org/10.3402/tellusb.v35i4.14612

Payandi-Rolland D, Shirokova L, Tesfa M et al (2020) Dissolved organic matter biodegradation along a hydrological continuum in permafrost peatlands. Sci Total Environ 749:141463. https://doi.org/10.1016/j.scitotenv.2020.141463

R Core Team (2019) R: a language and environment for statistical computing. R Foundation for Statistical Computing, Vienna, Austria

Raymond PA, Saiers JE, Sobczak WV (2016) Hydrological and biogeochemical controls on watershed dissolved organic matter transport: pulse-shunt concept. Ecology 97:5–16. https://doi.org/10.1890/14-1684.1

Rossel PE, Vähätalo AV, Witt M, Dittmar T (2013) Molecular composition of dissolved organic matter from a wetland plant (Juncus effusus) after photochemical and microbial decomposition (1.25 yr): Common features with deep sea dissolved organic matter. Org Geochem 60:62–71. https://doi.org/10.1016/j.orggeochem.2013.04.013

Roth V-N, Lange M, Simon C et al (2019) Persistence of dissolved organic matter explained by molecular changes during its passage through soil. Nat Geosci 12:755–761. https://doi.org/10.1038/s41561-019-0417-4

Schulz H, Popp P, Huhn G, Stärk H-J, Schüürmann G (1999) Biomonitoring of airborne inorganic and organic pollutants by means of pine tree barks. I. Temporal and spatial variations. Sci Total Environ 232:49–58. https://doi.org/10.1016/s0048-9697(99)00109-6

Shanley CS, Pyare S, Goldstein MI et al (2015) Climate change implications in the northern coastal temperate rainforest of North America. Clim Change 130:155–170. https://doi.org/10.1007/s10584-015-1355-9

Shirokova LS, Chupakov AV, Zabelina SA et al (2019) Humic surface waters of frozen peat bogs (permafrost zone) are highly resistant to bio-and photodegradation. Biogeosciences 16:2511–2526. https://doi.org/10.5194/bg-16-2511-2019

Smith HJ, Tigges M, D'Andrilli J, Parker A, Bothner B, Foreman C (2018) Dynamic processing of DOM: insight from exometabolomics, fluorescence spectroscopy, and mass spectrometry. Limnol Oceanogr Lett 3:225–235. https://doi.org/10.1002/lol2.10082

Spencer RG, Guo W, Raymond PA, Dittmar T, Hood E, Fellman J, Stubbins A (2014) Source and biolability of ancient dissolved organic matter in glacier and lake ecosystems on the Tibetan Plateau. Geochim Cosmochim Acta 142:64–74. https://doi.org/10.1016/j.gca.2014.08.006

Stenson AC, Marshall AG, Cooper WT (2003) Exact masses and chemical formulas of individual Suwannee River fulvic acids from ultrahigh resolution electrospray ionization Fourier transform ion cyclotron resonance mass spectra. Anal Chem 75:1275–1284. https://doi.org/10.1021/ac026106p

Stubbins A, Dittmar T (2012) Low volume quantification of dissolved organic carbon and dissolved nitrogen. Limnol Oceanogr: Methods 10:347–352. https://doi.org/10.4319/lom.2012.10.347

Stubbins A, Hood E, Raymond PA et al (2012) Anthropogenic aerosols as a source of ancient dissolved organic matter in glaciers. Nat Geosci 5:198. https://doi.org/10.1038/NGEO1403

Stubbins A, Silva LM, Dittmar T, Van Stan JTI (2017) Molecular and optical properties of tree-derived dissolved organic matter in throughfall and stemflow from live oaks and eastern red cedar. Front Earth Sci 5:22. https://doi.org/10.3389/feart.2017.00022

Tang Y, Horikoshi M, Li W (2016) ggfortify: unified interface to visualize statistical results of popular R packages. R J 8:474

Tejesvi MV, Mahesh B, Nalini MS, Prakash HS, Kini KR, Subbiah V, Shetty HS (2005) Endophytic fungal assemblages from inner bark and twig of Terminalia arjuna W. & A. (Combretaceae). World J Microbiol Biotechnol 21:1535–1540. https://doi.org/10.1007/s11274-005-7579-5

Textor S, Wickland K, Podgorski D, Johnston SE, Spencer RGM (2019) Dissolved organic carbon turnover in permafrost-influenced watersheds of interior Alaska: molecular insights and the priming effect. Front Earth Sci 7:275. https://doi.org/10.3389/feart.2019.00275

Thieme L, Graeber D, Hofmann D et al (2019) Dissolved organic matter characteristics of deciduous and coniferous forests with variable management: different at the source, aligned in the soil. Biogeosciences 16. https://doi.org/10.5194/bg-16-1411-2019

Van Stan JT, Wagner S, Guillemette F, Whitetree A, Lewis J, Silva L, Stubbins A (2017) Temporal dynamics in the concentration, flux, and optical properties of tree-derived dissolved organic matter in an epiphyte-laden oak-cedar forest. J Geophys Res: Biogeosci 122:2982–2997. https://doi.org/10.1002/2017JG004111

Van Stan JT, Stubbins A (2018) Tree-DOM: dissolved organic matter in throughfall and stemflow. Limnol Oceanogr Lett. https://doi.org/10.1002/lol2.10059

Vonk J, Tank S, Mann P et al (2015). Biodegradability of Dissolved Organic Carbon in Permafrost Soils and Waterways: a Meta-Analysis. https://doi.org/10.5194/bgd-12-8353-2015

Waggoner DC, Chen H, Willoughby AS, Hatcher PG (2015) Formation of black carbon-like and alicyclic aliphatic compounds by hydroxyl radical initiated degradation of lignin. Org Geochem 82:69–76. https://doi.org/10.1016/j.orggeochem.2015.02.007

Waggoner DC, Hatcher PG (2017) Hydroxyl radical alteration of HPLC fractionated lignin: formation of new compounds from terrestrial organic matter. Org Geochem 113:315–325. https://doi.org/10.1016/j.orggeochem.2017.07.011

Wagner S, Brandes J, Spencer RG, Ma K, Rosengard SZ, Moura JMS, Stubbins A (2019a) Isotopic composition of oceanic dissolved black carbon reveals non-riverine source. Nat Commun 10:1–8. https://doi.org/10.1038/s41467-019-13111-7

Wagner S, Fair JH, Matt S et al (2019b) Molecular hysteresis: hydrologically driven changes in riverine dissolved organic matter chemistry during a storm event. J Geophys Res: Biogeosci 124:759–774. https://doi.org/10.1029/2018JG004817

Xu B, Cao J, Hansen J et al (2009) Black soot and the survival of Tibetan glaciers. Proc Natl Acad Sci 106:22114–22118. https://doi.org/10.1073/pnas.0910444106

Xu Y, Xiao H, Guan H, Long C (2018) Monitoring atmospheric nitrogen pollution in Guiyang (SW China) by contrasting use of Cinnamomum Camphora leaves, branch bark and bark as biomonitors. Environ Pollut 233:1037–1048. https://doi.org/10.1016/j.envpol.2017.10.005

Publisher's Note Springer Nature remains neutral with regard to jurisdictional claims in published maps and institutional affiliations.